JOURNAL OF BACTERIOLOGY, Oct. 1992, p. 6608–6616
0021-9193/92/206608-09$02.00/0

Vol. 174, No. 20

Structural Characterization of Ordered Arrays of *sn*-Glycerol-3-Phosphate Acyltransferase from *Escherichia coli*

WILLIAM O. WILKISON,[1]† ROBERT M. BELL,[1] KENNETH A. TAYLOR,[2] AND M. JOSEPH COSTELLO[3]*

Departments of Biochemistry[1] and Cell Biology,[2] Duke University Medical Center, Durham, North Carolina 27710, and Department of Cell Biology and Anatomy, University of North Carolina at Chapel Hill, Chapel Hill, North Carolina 27599[3]

Received 16 January 1992/Accepted 7 August 1992

Overproduction of the *sn*-glycerol-3-phosphate acyltransferase in *Escherichia coli* leads to incorporation of this integral membrane protein into ordered tubular arrays within the cell. Freeze-fracture-etch shadowing was performed on suspensions of partially purified tubules and whole bacteria. This procedure revealed the presence of ridges and grooves defining a set of long-pitch left-handed helical ridges. The long-pitch helices represented chains of acyltransferase dimers. Tubules observed within the cell were often closely packed, with an apparent alignment of grooves and ridges in adjacent tubules. Fracture planes passing through the tubules indicated the presence of a bilayer structure, with some portion of the enzyme being associated with the membrane. The major portion of the enzyme extended from the hydrophilic surface, forming a large globular structure that, in favorable views, displayed a central cavity facing the cytoplasm. Computer analysis of shadowed tubules revealed that the left-handed helices were six stranded, with a pitch of 1,050 Å (105.0 nm) and a spacing of 75 Å (7.5 nm) between acyltransferase dimers along the chains. Analysis of the predicted secondary structure failed to reveal obvious transmembrane segments, suggesting that very little of the protein was inserted into the bilayer.

sn-Glycerol 3-phosphate (glycerol-P) acyltransferase catalyzes the transfer of an activated fatty acyl chain to the 1 position of *sn*-glycerol-3-phosphate, the first committed step in phospholipid biosynthesis in *Escherichia coli*. This integral membrane protein has been purified to homogeneity and shown to be a single polypeptide that migrates at 83 kDa on sodium dodecyl sulfate-polyacrylamide gels (15). The gene encoding this enzyme has been cloned and sequenced (18), revealing an open reading frame coding for a polypeptide of 91,260 daltons (17). Besides this sequence information, little is known about the molecular characteristics or structure of this important enzyme.

The glycerol-P acyltransferase was overexpressed in *E. coli* to very high levels by use of the appropriate plasmid vectors (29). Induction of glycerol-P acyltransferase synthesis caused the formation of intracellular tubular structures. These tubules were purified and shown to contain glycerol-P acyltransferase and phospholipid as the predominant components. Initial structural characterization by negative-stain electron microscopy revealed that the tubules were ordered helical arrays of the enzyme (29). This is the only known example of a crystalline array of a phospholipid biosynthetic enzyme.

A more detailed structural analysis of the negatively stained tubules was hindered by tubule flattening, dehydration artifacts, disordering of the helix, and overlapping of the two sides of the tubules, which made the interpretation of images and diffraction patterns difficult and ambiguous. Moreover, negative staining generally does not allow the determination of the handedness of a helix (10). To overcome these limitations and to extend the structural analysis, we examined tubules by using metal-shadowing techniques.

As determined by the freeze fracture-etch shadowing experiments and image analysis reported in this paper, the tubules are composed of chains of glycerol-P acyltransferase dimers having a long-pitch left-handed helical repeat of 1,050 Å (1 Å = 0.1 nm) and a subunit-to-subunit spacing of 75 Å along the chains. Shadowing of fractured and etched *E. coli* cells with thin layers of tantalum metal demonstrated that the ordered arrays of the enzyme are present in situ and that adjacent tubules are closely packed within the cytoplasm.

(This work was performed by W.O.W. in partial fulfillment of the requirements for the Ph.D. degree from Duke University Medical Center, Durham, N.C., 1988.)

MATERIALS AND METHODS

Specimen preparation. The plasmid-carrying bacterial strain used in this study (ORV30/pWW20) was previously described (29). Glycerol-P acyltransferase overproduction was induced with 5 mM isopropyl-β-D-thiogalactopyranoside as described previously (29), and whole cells were harvested at 4,000 × *g* for 10 min at 4°C, washed once with glass-distilled deionized water, and resuspended in a 1/10 volume of 20 mM sodium phosphate (pH 8.0). The cells were then frozen and processed as described previously (3). Tubule-enriched fractions (1 to 2 mg of protein per ml) were prepared from *E. coli* ORV30/pWW20 as previously described (29), except that the final pellet was resuspended in 20 mM sodium phosphate (pH 8.0).

Thin-section electron microscopy. Tubule-enriched fractions were washed in 0.1 M cacodylate buffer (pH 7.2) (solution A) and suspended in Karnovsky's fixative (9) for 2 h at 4°C. Samples were centrifuged at 10,000 × *g* for 30 min and washed in solution A. The pellet of tubules was resuspended in OsO_4 (2% final concentration) in solution A and

* Corresponding author.
† Present address: Glaxo Research Inc., Research Triangle Park, NC 27709.

placed on ice in the dark for 2 h. The sample was then washed with 0.85% sodium chloride (solution B) twice and resuspended in 0.5% uranyl acetate in solution B overnight at 4°C. Following overnight incubation, the sample was washed twice with solution B and dehydrated with an increasing ethanol series. The pellet was then embedded in Epon 812. Sections with gray interference were adsorbed onto carbon-coated grids for observation. All solutions were prepared in deionized glass-distilled water. Thin-section images were recorded with a JEOL 100CX electron microscope operated at 80 kV.

Freeze-fracture-etch shadowing. Small aliquots (0.05 to 0.1 μl) of tubule-enriched fractions or whole cells were frozen, fractured, and shadowed as described previously (3). Isolated tubules were processed in a Balzers 360 M vacuum chamber at −90°C, etched for 30 to 60 s, and replicated with platinum-carbon approximately 15 to 20 Å thick. Etching was about 50 to 100 nm deep, enough to reveal whole tubules suspended above roughened surfaces of ice and the copper sample supports. Whole cells were fractured and etched for 30 s at −100°C in a Leica (Reichert-Jung) Cryofract 190 vacuum chamber and replicated at −120°C with a layer of tantalum metal approximately 7 Å thick (2). For both instruments, the shadow inclination angle was 25°C, and metal thicknesses were recorded with quartz thin-film monitors. Replicas were processed such that the orientation of the sample was known (3). Electron micrographs were recorded with Philips 301, Philips 420, and JEOL 200CX transmission electron microscopes operated at 60 to 100 kV. Magnification corrections were made with a calibration grid with 2,160 lines per cm. Images were photographically reversed to produce black shadows (8), and the shadow direction is noted on the micrographs.

Image processing. Micrographs of both shadowed and negatively stained tubules were selected for image processing by visual inspection. Generally, the shadowed tubules were straight over lengths of 0.2 to 0.5 μm in the replicas. The selected micrographs were digitized on a Perkin-Elmer PDS 1010M microdensitometer at a step size of 6 to 10 Å with respect to the original tubules. For the shadowed tubules, the digitized image was rotated by bilinear interpolation so that the tubule axis ran parallel to the vertical sampling axis. The tubules were then windowed from the optical density matrix, edge apodized, and transformed (24). The Fourier transform of the image usually revealed two and sometimes as many as four nonequatorial layer lines. Filtered images were obtained by masking of each layer line and then by computing the reverse transformation. The masking was performed on the Fourier transform by use of rectangular holes with dimensions of 0.0093 by 0.004 $Å^{-1}$.

Negatively stained tubules were rarely straight and were thus subjected to an image-straightening protocol kindly provided by M. F. Schmid. In brief, this protocol entailed determination of the center of the filament axis and then bicubic spline interpolation to correct for curvature. These straightened filaments rarely yielded detailed Fourier transforms. We believe that this lack of improvement was the result of the generally poor preservation of the tubules by negative staining, which appears to disrupt the helical structure. The poor helical order in the negatively stained tubules was thus not due to curvature alone and so could not be improved by computational means. For this reason, we based the diffraction analysis on the metal-shadowed specimens.

Miscellaneous methods. Membrane fractions or tubule-enriched fractions were measured for glycerol-P acyltransferase activities as previously described (7). Assays were performed (i) directly in the absence of added phospholipid vesicles, (ii) with the addition of phospholipid vesicles only, and (iii) by reconstitution into phospholipid vesicles (29) following Triton X-100 solubilization of membrane or tubule-enriched fractions. The protein concentration was determined by the method of Peterson (22). Sodium dodecyl sulfate-polyacrylamide gel electrophoresis was performed by the method of Laemmli (13). Negative-staining procedures were described previously (29). The hydropathy plot was made by the method of Kyte and Doolittle (12) with a window of 19 amino acids.

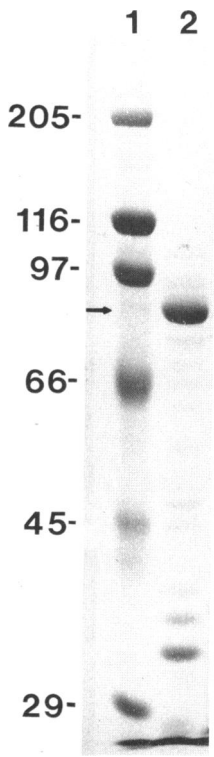

FIG. 1. Abundance of glycerol-P acyltransferase in tubule-enriched fractions. Tubules were isolated as described in Materials and Methods. Samples were electrophoresed in a 7.5% Laemmli gel and then stained with Coomassie blue. Lanes: 1, molecular mass standards (myosin, 205 kDa; β-galactosidase, 116 kDa; phophorylase *b*, 97.4 kDa; bovine serum albumin, 66 kDa; ovalbumin, 45 kDa; carbonic anhydrase, 29 kDa); 2, 25 μg of tubule-enriched fraction. Numbers on the left indicate molecular masses of standards. The arrow indicates the position at which authentic glycerol-P acyltransferase migrates.

RESULTS

Biochemical characterization of tubules. The tubule-enriched fraction isolated for these studies was subjected to sodium dodecyl sulfate-polyacrylamide gel electrophoresis (Fig. 1). The sample was highly enriched in glycerol-P acyltransferase, which accounted for approximately 80% of the polypeptide on the gel, as determined by densitometry (data not shown). Two other prominent polypeptides of 33 and 36 kDa and copurifying with the tubules accounted for 10 and 7%, respectively. These two proteins were most likely the OmpA and OmpB proteins, major components of the outer membrane, as suggested by the presence in the

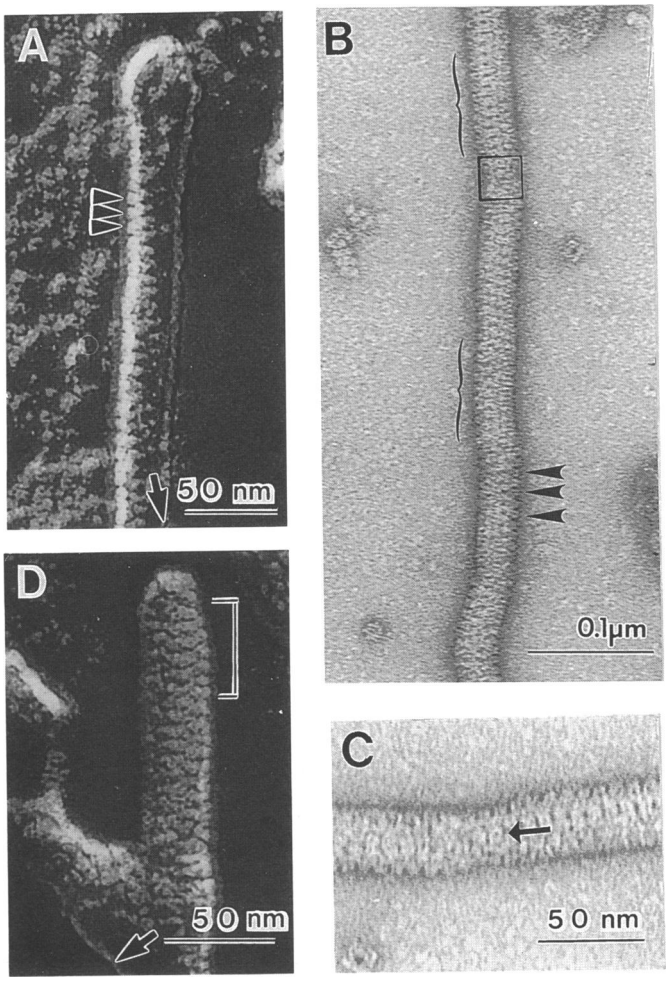

FIG. 2. Comparison of negatively stained and unidirectionally shadowed tubules. Tubules were processed as described in Materials and Methods. (A) Platinum-carbon-shadowed tubule. Arrowheads indicate subunits projecting from the side. The arrow near the scale marker here and in subsequent figures indicates the shadow direction. (B) Tubule negatively stained with 1% uranyl acetate. Arrowheads indicate subunits projecting from the side. The brackets indicate regions in which the side patterns were similar. (C) Higher-magnification view of boxed region in panel B. Note the distortion of the regular array when the side pattern alternated. The arrow indicates a circular subunit (see the text). (D) Shadowed tubule; the alternating side pattern is apparent. The bracket indicates a region in which a particular side pattern predominated.

preparation of structures that resembled outer membrane vesicles (30).

Measurements of glycerol-P acyltransferase activity revealed that, when the enzyme was packed in tubules, it was inactive (specific activity, <1 nmol/min/mg). The addition of phospholipid vesicles to tubules produced only modest specific activity (25 nmol/min/mg). However, solubilization of the glycerol-P acyltransferase in Triton X-100 and reconstitution into phospholipid vesicles resulted in very high specific activity (2.7 μmol/min/mg). This activity was only twofold lower than the activity of glycerol-P acyltransferase purified to homogeneity by the method of Green et al. (7). Particulate fractions prepared from the same bacterial strain had fivefold lower specific activity (555 nmol/min/mg) than the tubule fractions, suggesting some enrichment of the enzyme in the tubules.

Comparison of shadowed and negatively stained tubules. The overall appearance of shadowed tubules (Fig. 2A) was similar in many respects to that of tubules preserved by negative staining (Fig. 2B; see also reference 29). First, the edge structures had the same dimensions. The structures in the shadowed specimen measured 55 Å in projection from the edge of the tubule and were spaced 65 Å apart (Fig. 2A, arrowheads). The negatively stained structures were 55 Å in projection and were spaced 68 Å apart (Fig. 2B, arrowheads).

Second, the alternating side pattern noted previously by negative staining (29) was also observed in the shadowed tubules. The side structure morphology alternated approximately every 900 to 1,000 Å in negatively stained tubules of suitable length (Fig. 2B, brackets). At the point at which the side pattern switched, it appeared that the regular pattern observed was distorted dramatically (Fig. 2C). Similar patterns were observed for most of the shadowed tubules, although the straight portions of the tubules usually contained less than two repeats (Fig. 2D, bracket).

Third, individual subunits appeared to be equivalent in the two preparations. In negatively stained tubules, the subunit had an approximately circular shape, with a diameter of 65 Å, as viewed from the topmost aspect of the tubule (Fig. 2C,

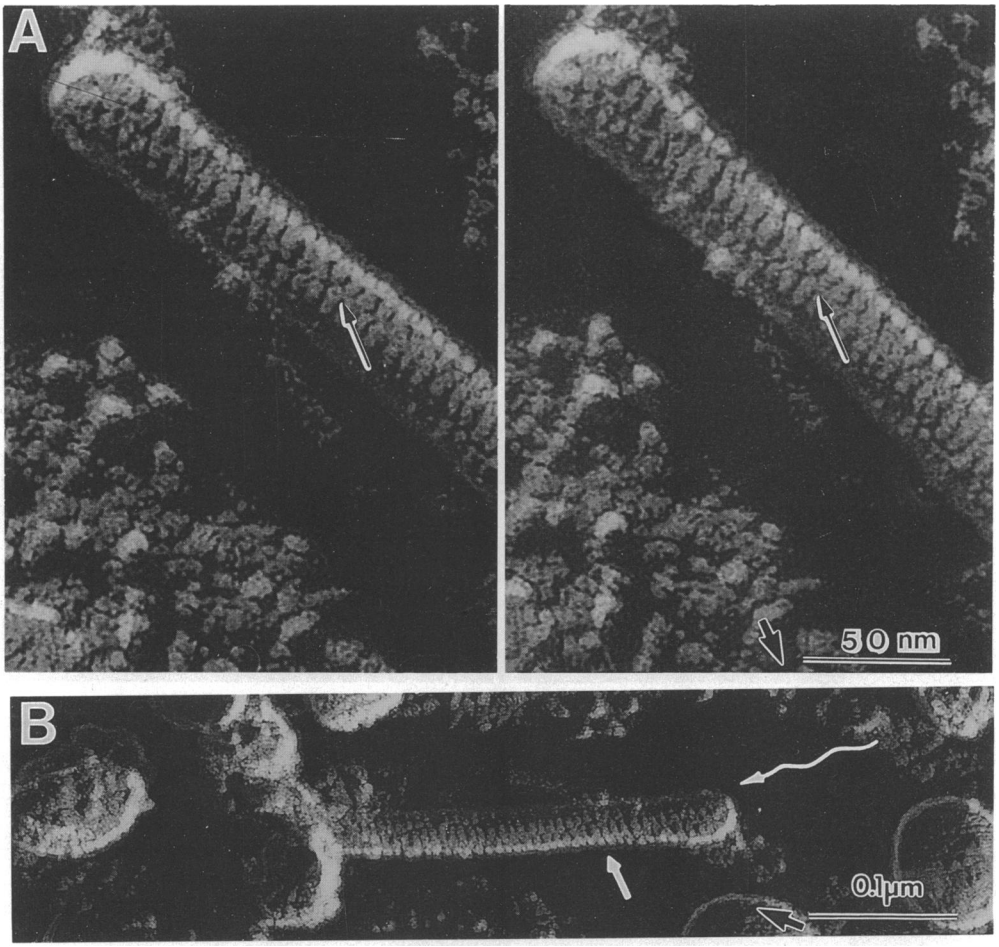

FIG. 3. Helical groove and subunit morphology in shadowed tubules. Tubules were isolated and shadowed as described in the legend to Fig. 2. (A) Stereo view of a shadowed tubule. The arrow on the tubule indicates the paired subunits from the topmost aspect of the tubule. Note the centrally located deposit of metal, suggesting that a cavity that is open to the cytosol exists. (B) Lower-magnification view of the same tubule. The wavy white arrow indicates the prominent left-handed helical groove apparent in this view. The straight white arrow shows the right-handed helical nature of the tubule.

arrow). A stain-included portion, measuring 27 Å in diameter, was located in the central region of the subunit (Fig. 2C, arrow). In shadowed tubules, the subunit also appeared to be circular, with a central cavity also apparent, indicating that this hole is open to the environment and not totally enclosed by protein (Fig. 3A, arrow). This subunit measured 68 Å in diameter.

Helical patterns. Heavy metal shadowing revealed aspects of the tubules that were not readily apparent in the images of negatively stained tubules. The most obvious difference was the appearance in most tubules of long-pitch left-handed helical grooves (Fig. 3B, wavy arrow; see also Fig. 2A and 3A). Measurements made directly from electron micrographs indicated that the long-pitch grooves were angled at 10 to 14°C with respect to the tubule axis. The grooves were least obvious when the shadow direction was parallel to the long axis of the tubule, as predicted from observations by others for shadowed helical structures (10). Short-pitch right-handed helices were also observed (Fig. 3B, straight arrow). Rotary metal shadowing of the tubules failed to reveal any additional aspects of the tubules (data not shown); in fact, the major difference observed was that the left-handed grooves were not as obvious as in unidirectionally shadowed structures.

Associations of subunits. The tubules contained helical arrays of individual enzyme molecules (or subunits). The individual molecules appeared to be associated in pairs, forming dumbbell-shaped dimeric structures (Fig. 3A). These dimers were evident throughout the structures but were most obvious on the topmost portion of the tubules. The helical packing was most easily recognized by following the pattern of the dimers. Chains of dimers formed a left-handed helical arrangement of ridges (Fig. 3B). Each tubule appeared to be composed of six chains of dimers, based on the diameter of the tubule (280 Å) and the width of the dimer chain (145 Å).

Tubular organization in situ. Previous observations of thin sections of whole cells indicated that individual tubules were associated in tightly packed bundles in situ (29). For studying the organization of these arrays, whole cells were fractured, etched, and shadowed with tantalum (2). Longitudinal fractures revealed the presence of tubular bundles (Fig. 4A). The bundles were often aligned along the long axis of the bacterium, in close association with the inner membrane.

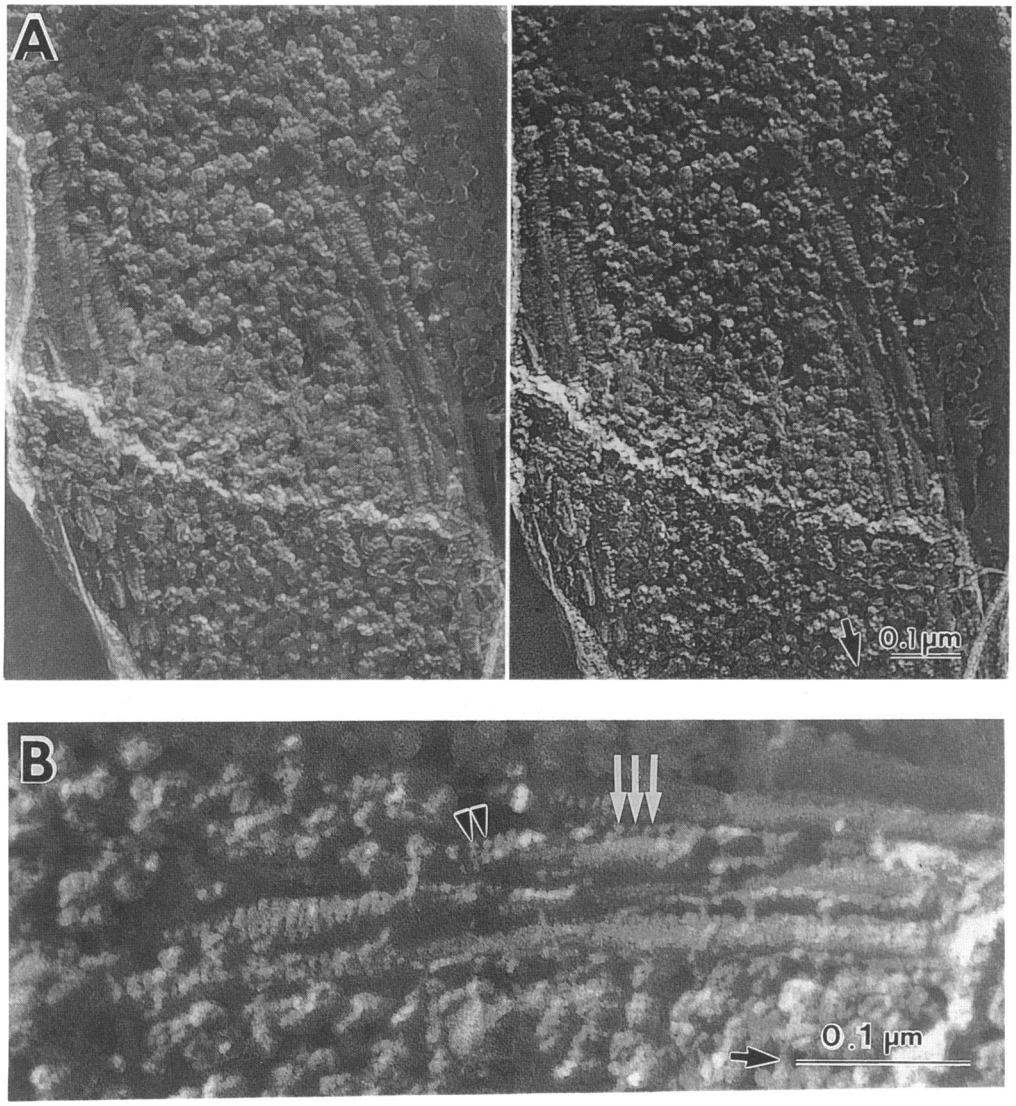

FIG. 4. In situ replica of tubular bundles. Induced whole cells were prepared and unidirectionally shadowed with tantalum as described in Materials and Methods. (A) Stereo view showing tubular bundles in close association with the cell envelope. (B) Higher-magnification view of the bundles of tubules on the right side of panel A. The white arrows and arrowheads indicate two different views of individual subunits on the edge of the fracture plane.

However, in some cases, the bundles traversed the cell at an approximate angle of 11° with respect to the long axis of the bacterium (data not shown). In tubules not split by the fracture plane, the tubules were closely packed, such that the ridges of one tubule appeared to fit into the grooves of its neighbors.

At a higher magnification, individual subunits could be discerned (Fig. 4B). They appeared to be 60-Å-wide globular structures attached to the surfaces of the tubules. In addition, some fracture planes occurred between the leaflets of the membrane bilayer, exposing a relatively smooth inner leaflet. The smooth inner leaflet suggested little or no insertion of the enzyme into this region. To determine whether transmembrane segments would be expected to occur in the glycerol-P acyltransferase, we performed a Kyte-Doolittle (12) analysis of the primary sequence (Fig. 5). Interestingly, the glycerol-P acyltransferase had no predicted transmembrane segments.

Thin sections of tubules. Cross sections of isolated tubules revealed a multilayered structure with an electron-translucent region measuring 70 Å in diameter and surrounded by a trilamellar pattern (Fig. 6). The central layer of the trilamellar pattern was lightly stained and was composed of 10 to 12 globular domains encircling the tubules (Fig. 6). On either side of this translucent band were darkly stained regions that each measured about 35 to 55 Å (Fig. 6). The overall diameter of the tubules averaged 240 ± 17 Å, a value similar to the value obtained for tubules examined in thin sections of whole bacteria (29). This diameter was probably reduced by dehydration during processing. The diameters of negatively stained tubules (275 to 335 Å) (29) and shadowed tubules (280 ± 15 Å for isolated tubules and 290 ± 16 Å for tubules shadowed in situ) were significantly larger than those of tubules in thin sections.

Image analysis of unidirectionally shadowed tubules. Fourier transform diffraction patterns for tubules shadowed with

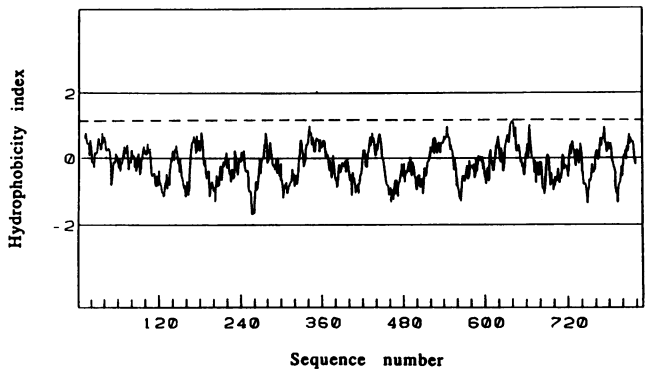

FIG. 5. Hydropathy plot of glycerol-P acyltransferase. The primary sequence of glycerol-P acyltransferase, as inferred from the gene sequence, was analyzed by the method of Kyte and Doolittle (12). Hydropathic index values (ordinate) were determined over an average of 19 residues (the abscissa shows amino acid residues). The broken line (at 1.2, based on analogous plots for bacteriorhodopsin; see reference 12) indicates where potential membrane-spanning segments should be observed. No portions of the sequence were sufficiently hydrophobic to cross the broken line. Thus, glycerol-P acyltransferase lacks predicted helical transmembrane segments.

tantalum (data not shown) or platinum-carbon (Fig. 7A and D) were qualitatively similar to those obtained for negatively stained tubules (29). A series of layer lines spaced at 1,050 Å were obtained. The innermost layer line arose from long-pitch left-handed helical grooves (Fig. 7B and E). A second set of layer lines (Fig. 7B and E) occurred at spacings of 75 and 65.3 Å and arose from the arrangement of protein dimers along the long-pitch helices. The axial spacing of the layer line at 75 Å is in reasonable agreement with that observed earlier for the layer line at 78 Å (29).

Tentatively, we assign the layer lines at 75 and 65.3 Å as the 14th and 16th layer lines on the basis of the observations that the radial separation of the peaks for these two layer lines is twice the radial distance to the peak for the 1st layer line and that the axial separation between these two layer lines is twice the axial position of the 1st layer line. The 15th layer line is thus predicted to be meridional. Its absence from the Fourier transform may be a systematic extinction or simply a low amplitude in the transform.

We have determined a tentative surface lattice based on the tubule dimensions and the limited data available from computed diffraction patterns (Fig. 7). On the basis of a tubule diameter of 280 Å, the axial and radial positions of peaks for the layer lines, and the assumption of six strands of dimers per tubule, a primitive unit cell with axial dimensions of 140 and 74 Å and an included angle of 80° can be obtained. With respect to the tubule axis, the longer axis is rotated by −72.1° and the shorter axis is rotated by 8°. The unit cell contains one glycerol-P acyltransferase dimer.

DISCUSSION

The detailed analysis of negatively stained tubules has been hampered because of the variability of the structure, caused in part by inherent irregularities in the packing of subunits and surface tension-induced deformations of the tubules. It is rare to observe straight tubules of any significant length by negative staining, whereas long stretches of straight tubules can be seen in frozen and shadowed specimens. The consistent values obtained for the diameter of the tubules (280 ± 15 Å for isolated tubules and 290 ± 16 Å for tubules shadowed in situ) also suggest that the packing of glycerol-P acyltransferase into tubules is a very precise process. In addition, as far as we can observe, the helical parameters of the tubules are variable only within narrow limits, suggesting that the tubules are well ordered in situ and when isolated in suspension. They become partially disordered during negative staining, thereby making it difficult to ascertain their helical structure.

With the technique of freeze-fracture-etch shadowing, the interpretation of optical diffraction data obtained from these structures has been simplified. The tubules contain six strands of glycerol-P acyltransferase dimers arranged in a left-handed helix with a repeat period of 1,050 Å. The separation between dimers in each strand is 74 Å. Previous studies of negatively stained tubules with optical diffraction of short lengths of tubules revealed a prominent nonequatorial layer line at an axial spacing of 78 Å and a meridional layer line at a spacing of 39 Å. The layer line observed earlier at 78 Å (29) probably represents the layer line observed in the present work at 75 Å. The very short lengths of tubules used earlier would have made impossible the separation of the layer line at 65.3 Å from the layer line at 75 Å. However,

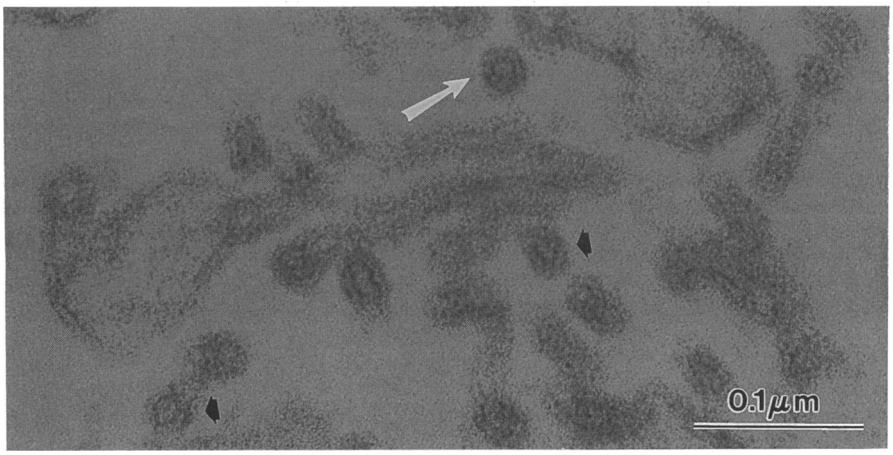

FIG. 6. Cross-sectional view of isolated tubules. Tubule-enriched fractions were isolated and processed for thin-section analysis as described in Material and Methods. Arrows indicate different cross-sectional views; the best view is indicated by the white arrow.

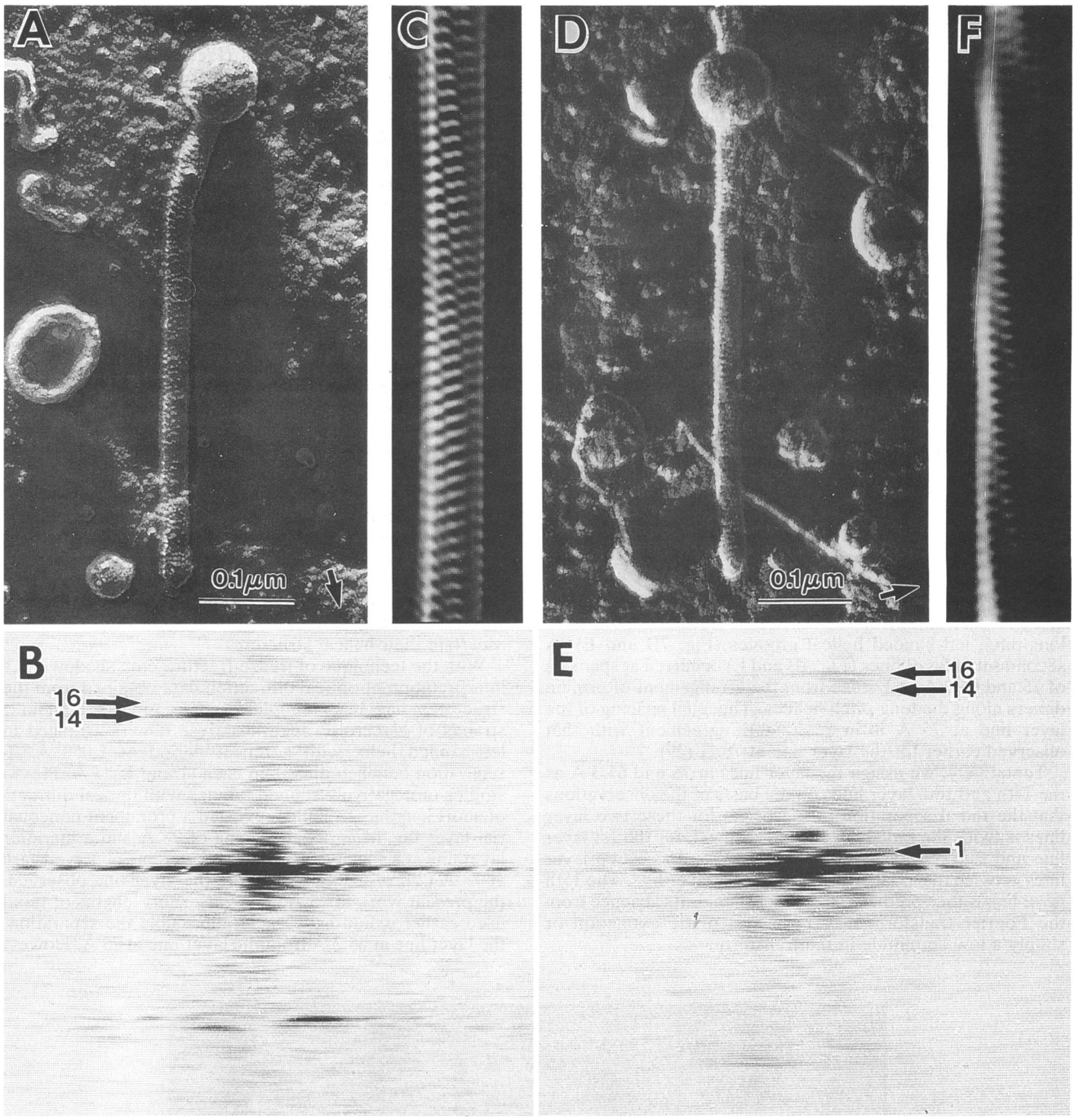

FIG. 7. Image analysis of unidirectionally shadowed tubules. (A and D) Nearly straight tubules shadowed with platinum-carbon in different shadowing directions. In panel A, the shadowing direction is nearly parallel to the tubule axis, thereby enhancing the contrast due to the glycerol-P acyltransferase dimers. In panel D, the shadowing direction is nearly perpendicular to the tubule axis, thereby enhancing the long-pitch left-handed helix. (B and E) Diffraction patterns revealing the set of layer lines arising from the tubules. The innermost layer line (labeled 1) in panel E arose from a left-handed helix with a pitch of 1,050 Å. (C and F) Filtered images revealing the arrangement of glycerol-P acyltransferase dimers. In panel C, the dimers are well delineated, and in panel F, the long-pitch helical grooves of the dimers are emphasized.

a more detailed analysis of the diffraction patterns will probably require micrographs of frozen hydrated tubules (suspended in amorphous ice) because of the considerable disordering that seems to occur in negative staining and the limited resolution available for metal-shadowed tubules.

The six strands of dimers observed are consistent with the 10 to 12 subunits observed in thin-section images of tubule cross sections and the 10 or 11 subunits per turn reported previously (29).

Tantalum shadowing of tubules in situ not only produced

some information regarding the organization of tubular bundles but also revealed important details about the structure of individual glycerol-P acyltransferase molecules. For subunits located at the edge of a fracture plane and in the proper orientation with respect to the direction of shadowing, the enzyme appears to have a distinct morphology consisting of a large globular domain extending from the tubule surface into the cytoplasm. Several integral transmembrane proteins, such as ATP synthetase (26), fumarate reductase (16), 3-hydroxy-3-methylglutaryl coenzyme A reductase (19), the acetylcholine receptor (25), and Na^+,K^+-ATPase (31), have a similar highly asymmetric association with membranes and have been demonstrated to form tubular structures similar to those of glycerol-P acyltransferase. Crystalline tubules of the acetylcholine receptor have some features in common with tubules of glycerol-P acyltransferase, in that the receptor is packed in helical arrays of dimers, with the large domain extending from the tubule surface (25). In the case of Na^+, K^+-ATPase, it has been postulated that the formation of helical tubular intermediates during in situ crystallization of this enzyme may be driven by the interactions of the relatively large cytoplasmic regions and the smaller hydrophobic domains (31). It is possible that glycerol-P acyltransferase tubules are formed in an analogous manner.

The absence of obvious pits in the inner leaflet of tubules freeze-fractured in situ (Fig. 4) suggests that glycerol-P acyltransferase may not penetrate deeply into the phospholipid bilayer. Consistent with this hypothesis is the absence of predicted transmembrane segments in a computer analysis done by the method of Kyte and Doolittle (12; Fig. 5). The amount of protein within the bilayer may thus be even lower than the 18 to 37% estimated previously (29) on the basis of assumptions about the composition of the tubules and limited structural data. However, there is strong evidence that this enzyme is an integral membrane protein, as indicated by its absolute requirement of phospholipid for activity (7), the necessity of a detergent for solubilization from the membrane (11), and the colocalization of proteolytic fragments with phospholipid vesicles (6). Therefore, it is likely that the tubules are organized as a cytoplasmic array of the enzyme, with only a small portion of the protein bound to the surface or inserted into the phospholipid bilayer.

Most of the tubules observed terminated either by gradual tapering of the end (Fig. 2D) or by merging into a spherical vesicle with a diameter larger than that of the tubule (Fig. 2A and 7A and D). Similar end features were reported for tubules of the acetylcholine receptor (25). For glycerol-P acyltransferase tubules, we suspect that the vesicular ends were portions of the *E. coli* inner membrane that were isolated with the tubules. In cases in which the tubule end had the same or a smaller diameter than the tubule, the end (or cap) appeared to be composed of the same material. The protein contacts necessary for a helical assembly would not favor collapse into a sealed end (1). In many helical systems, such as the f1 bacteriophage capsid, the ends of the helical protein coat are capped by different proteins (27), and mutations in the genes coding for these end proteins cause the formation of longer-than-normal coats known as polyphage (20). Also, mutations in other bacteriophage coat protein genes allow the formation of tubular structures known as polyheads, composed primarily of the major capsid protein, instead of the normal icosahedral heads (4, 21), suggesting that a separate protein with different contacts is necessary to cap the helix. Therefore, it is possible that glycerol-P acyltransferase tubules are capped by some end protein needed to terminate the helix.

Tubule morphogenesis bears many similarities to bacteriophage assembly. In phage T4, the major coat protein exists as a membrane-bound protein until assembly on the inner membrane to form the head (23). Since glycerol-P acyltransferase is an inner membrane protein in *E. coli*, it is possible that the assembly of tubules occurs by a similar mechanism. In addition, mutations in a heat shock gene, *groEL*, cause the major coat protein of T4 to aggregate into inclusion bodies (14). We have shown that tubule formation is blocked in *E. coli* deficient in the heat shock response, resulting instead in the appearance of inclusion bodies (28). This result raises the possibility that heat shock proteins, or chaperones (5), are necessary for the assembly of the tubules. Therefore, glycerol-P acyltransferase tubule formation may constitute a simple system for the study of assembly processes in general.

ACKNOWLEDGMENTS

This work was supported by Public Health Service grants GM20015 (R.M.B. and W.O.W.) and GM30598 (K.A.T.) from the National Institute of General Medical Sciences.

We gratefully acknowledge the technical assistance of Gerda Vegara with the thin sections.

REFERENCES

1. **Casjens, S.** 1985. Overview of viral assembly, p. 5–7. *In* S. Casjens (ed.), Virus structure and assembly. Jones and Bartlett Publishers, Inc., Boston.
2. **Costello, M. J., and J. Escaig.** 1989. Preparation of thin, fine-grained tantalum replicas for freeze-fracture electron microscopy. Scanning Microsc. Suppl. **3**:189–200.
3. **Costello, M. J., and R. D. Fetter.** 1986. Freeze-fracture methods: preparation of complementary replicas for evaluating intracellular ice damage in ultrarapidly cooled specimens. Methods Enzymol. **12**:704–718.
4. **Cummings, D. J., V. A. Chapman, S. S. DeLong, and A. R. Kusy.** 1971. Structural aberrations in T-even bacteriophage. II. Characterization of the proteins contained in aberrant heads. Virology **44**:425–442.
5. **Ellis, R. J., and S. M. van der Vies.** 1991. Molecular chaperones. Annu. Rev. Biochem. **60**:321–347.
6. **Green, P. R., and R. M. Bell.** 1984. Asymmetric reconstitution of homogeneous *Escherichia coli sn*-glycerol-3-phosphate acyltransferase into phospholipid vesicles. J. Biol. Chem. **259**: 14688–14694.
7. **Green, P. R., A. H. Merrill, Jr., and R. M. Bell.** 1981. Membrane phospholipid synthesis in *Escherichia coli*. Purification, reconstitution, and characterization of sn-glycerol-3-phosphate acyltransferase. J. Biol. Chem. **256**:11151–11159.
8. **Heuser, J.** 1981. Preparing biological samples for stereomicroscopy by the quick-freeze, deep-etch, rotary-replication technique. Methods Cell Biol. **22**:97–122.
9. **Karnovsky, J. M.** 1965. A formaldehyde-glutaraldehyde fixative of high osmolarity for use in electron microscopy. J. Biophys. Biochem. Cytol. **11**:729–732.
10. **Kensler, R. W., and R. J. C. Levine.** 1982. Determination of the handedness of the crossbridge helix of *Limulus* thick filaments. J. Muscle Res. Cell Motil. **3**:349–361.
11. **Kessels, J. M. M., and H. Van Den Bosch.** 1982. Characterization of reconstituted partially purified glycerophosphate acyltransferase from *Escherichia coli*. Biochim. Biophys. Acta **713**:570–580.
12. **Kyte, J., and R. F. Doolittle.** 1982. A simple method for displaying the hydropathic character of a protein. J. Mol. Biol. **157**:105–132.
13. **Laemmli, U. K.** 1970. Cleavage of structural proteins during the assembly of the head of bacteriophage T4. Nature (London) **227**:680–685.
14. **Laemmli, U. K., F. Beguin, and G. Gujer-Kellenberger.** 1971. A factor preventing the major head protein of bacteriophage T4 from random aggregation. J. Mol. Biol. **47**:69–85.

15. **Larson, T. J., V. A. Lightner, P. R. Green, P. Modrich, and R. M. Bell.** 1980. Membrane phospholipid synthesis in *Escherichia coli*. Identification of the *sn*-glycerol-3-phosphate acyltransferase polypeptide as the *plsB* gene product. J. Biol. Chem. **255:**9421–9426.
16. **Lemire, B. D., J. J. Robinson, R. D. Dradley, D. G. Scraba, and J. H. Weiner.** 1983. Structure of fumarate reductase on the cytoplasmic membrane of *Escherichia coli*. J. Bacteriol. **155:** 391–397.
17. **Lightner, V. A., R. M. Bell, and P. Modrich.** 1983. The DNA sequences encoding *plsB* and *dqk* loci of *Escherichia coli*. J. Biol. Chem. **258:**10856–10861.
18. **Lightner, V. A., T. J. Larson, P. Tailleur, G. D. Kantor, C. R. H. Raetz, R. M. Bell, and P. Modrich.** 1980. Membrane synthesis in *Escherichia coli*. Cloning of a structural gene (*plsB*) of the *sn*-glycerol-3-phosphate acyltransferase. J. Biol. Chem. **255:**9413–9420.
19. **Liscum, L., J. Finer-Moore, R. M. Stroud, K. L. Luskey, M. S. Brown, and J. L. Goldstein.** 1985. Domain structure of 3-hydroxy-3-methylglutaryl coenzyme A reductase, a glycoprotein of the endoplasmic reticulum. J. Biol. Chem. **260:**522–530.
20. **Lopez, J., and R. E. Webster.** 1983. Morphogenesis of filamentous bacteriophage f1: orientation of extrusion and production of polyphage. Virology **127:**177–190.
21. **Murialdo, H., and L. Simonovitch.** 1972. The morphogenesis of phage lambda. V. Form-determining function of the genes required for assembly of the head. Virology **48:**822–835.
22. **Peterson, G. L.** 1977. A simplification of the protein assay method of Lowry et al. which is more generally applicable. Anal. Biochem. **83:**346–356.
23. **Simon, L. D.** 1972. Infection of *Escherichia coli* by T2 and T4 bacteriophages as seen in the electron microscope: T4 head morphogenesis. Proc. Natl. Acad. Sci. USA **69:**907–911.
24. **Taylor, K. A., M.-H. Ho, and A. Martonosi.** 1986. Image analysis of the Ca^{2+}-ATPase from sarcoplasmic reticulum. Ann. N.Y. Acad. Sci. **483:**31–43.
25. **Unwin, N., C. Toyoshima, and E. Kubalek.** 1988. Arrangement of the acetylcholine receptor subunits in the resting and desensitized states, determined by cryoelectron microscopy of crystallized *Torpedo* postsynaptic membranes. J. Cell Biol. **107:** 1123–1138.
26. **von Meyenburg, K., B. B. Jorgensen, and B. van Deurs.** 1984. Physiological and morphological effects of overproduction of membrane-bound ATP synthetase in *Escherichia coli* K-12. EMBO J. **8:**1791–1797.
27. **Webster, R. E., and J. Lopez.** 1985. Structure and assembly of the class I filamentous bacteriophage, p. 257–258. *In* S. Casjens (ed.), Virus structure and assembly. Jones and Bartlett Publishers, Inc., Boston.
28. **Wilkison, W. O., and R. M. Bell.** 1988. *sn*-Glycerol-3-phosphate acyltransferase tubule formation is dependent upon heat shock proteins (*htpR*). J. Biol. Chem. **263:**14505–14510.
29. **Wilkison, W. O., J. P. Walsh, J. M. Corless, and R. M. Bell.** 1986. Crystalline arrays of the *Escherichia coli sn*-glycerol-3-phosphate acyltransferase, an integral membrane protein. J. Biol. Chem. **261:**9951–9958.
30. **Yamato, I., Y. Anraku, and K. Kirosawa.** 1975. Cytoplasmic membrane vesicles of *Escherichia coli*. I. A simple method for preparing the cytoplasmic and outer membranes. J. Biochem. **77:**705–718.
31. **Zampighi, G., J. Kyte, M. Kreman, and S. A. Simon.** 1985. One dimensional crystals of Na^+, K^+-ATPase dimers. Biochim. Biophys. Acta **854:**45–57.